

APPLICATION OF HEUN'S CONFLUENT EQUATION FOR THE SOLUTION OF THE HYDROGEN ATOM PROBLEM IN SPHEROIDAL COORDINATES

T. Kereselidze^{1*}, G. Chkadua² and J. F. Ogilvie^{3,4}

¹Faculty of Exact and Natural Sciences, Tbilisi State University, Chavchavadze Avenue 3, 0179 Tbilisi, Georgia.

²Department of Mathematics, King's College London, Strand, London, WC2R 2LS, United Kingdom

³Escuela de Química, Universidad de Costa Rica, Ciudad Universitaria Rodrigo Facio, San Pedro de Montes de Oca 11501-2050, San Jose, Costa Rica

⁴Centre for Experimental and Constructive Mathematics, Department of Mathematics, Simon Fraser University, 8888 University Drive, Burnaby, British Columbia V5A 1S6 Canada

Abstract.

The Schrödinger equation in prolate spheroidal coordinates separates into ordinary-differential equations in single coordinates; of these direct solutions, two contain confluent Heun functions. We derive polynomial solutions of Heun's confluent equation and express Coulomb spheroidal functions in a closed algebraic form. Spheroidal orbitals are expressible as hybrids composed of spherical ones corresponding to a degenerate level. The contribution of each spherical orbital within a hybrid orbital depends on distance R from a nucleus to a dummy centre, and varies substantially with R . The most stretched orbitals are either toward a dummy centre having quasi-angular nodes of maximum number or in the opposite direction for an orbital having quasi-radial nodes of maximum number. For the purpose of direct applications of the wave functions of hydrogen in molecular physics, wave functions expressed in spheroidal coordinates are the most useful.

Keywords: hydrogen atom; spheroidal coordinates; Coulomb spheroidal orbitals;

1. Introduction

The solution of the Schrödinger equation for the hydrogen atom is of such fundamental importance that its solutions must be found in all possible cases. The problem is typically treated in spherical polar and paraboloidal coordinates in textbooks of quantum mechanics in physics [1]. The solution involves separating the spherical or paraboloidal variables so that the amplitude or wave functions are represented as a product of the one-dimensional functions.

In addition to spherical polar and paraboloidal coordinates, the Schrödinger equation for the hydrogen atom is separable in prolate spheroidal coordinates. An atomic nucleus is located at one focus of those spheroidal coordinates; another focus is at distance R from the nucleus. The separation yields three equations for the three spatial variables, which become the familiar radial and angular equations when R tends to zero; their solutions might hence be called quasi-radial and quasi-angular functions. The interest in the solution of the hydrogen atom in spheroidal coordinates arises because it is closely related to the so-called two-Coulomb-centre problem (an electron moving in the field of two fixed Coulomb centres with charges Z_1 and Z_2) for which the Schrödinger equation is separable also in prolate spheroidal coordinates. In the case in which $Z_1 = Z_2 = 1$, i.e. for hydrogen molecular ion H_2^+ , the problem was treated by Pauli [2] on the basis of the old Bohr quantum theory before the development of quantum mechanics. Among the first quantum-mechanical considerations, one

*Corresponding author; e-mail address: tamaz.kereselidze@tsu.ge

treatment of H_2^+ was undertaken by Wilson [3,4], who thought that the solutions of the one-dimensional equations obtained after separation of spheroidal variables in the Schrödinger equation

might be represented in a polynomial form. In his paper Teller [5] indicated that, although the expansions introduced by Wilson for the solutions converged, these expansions are not representable in a polynomial form. Bates and Read [6] undertook a detailed study of H_2^+ ; for arbitrary Z_1 and Z_2 , the solution of the problem is found, e.g., in the paper of Power [7]. As the wave functions of the Z_1eZ_2 system are basic to all molecular physics and quantum chemistry, it becomes evident that knowledge of the explicit algebraic expressions for the hydrogenic wave functions in spheroidal coordinates is highly desirable.

Coulson and Robinson [8] made initial attempts to solve the problem of the hydrogen atom in spheroidal coordinates; their important result was a termination of the power series for the one-dimensional functions and a derivation of Coulomb spheroidal functions (CSF) for some low-lying eigenstates in a polynomial form. Cook and Fowler [9] have used these techniques to extend the known solutions and study their application to the theory of chemical bonding. They presented contour diagrams of CSF at selected values of R . Using the *hidden symmetry* of the hydrogen atom, Sung and Hercshbach [10] derived CSF for eigenstates with $n \leq 4$ and $m \leq 4$ (n denotes the principal quantum number; m denotes the modulus of the magnetic quantum number). For eigenstates with $m=0$, Coulomb elliptic wave functions are obtained and used for study molecular Rydberg states [11]. With a suggested simple and straightforward scheme of calculation [12], CSF are derivable in principle for arbitrary eigenstates. Despite substantial progress, a general solution of the problem in spheroidal coordinates is lacking, mostly because solutions of the appropriate one-dimensional equations were not recognized to be expressible in terms of known special functions. With two exceptions [9,10] the graphs of CSF have not been reported.

An isolated atom is the only system in which a model based on spherical symmetry would be at all realistic. Because the presence of a second attracting centre in a diatomic molecule distorts the field, the deviation from spherical symmetry must be taken into account. A theory of the electronic structure of diatomic molecules hence requires a set of atomic wave functions that reflect not just the static spatial symmetry of an atom but the dynamical properties of atomic orbitals. It is assumed that a lack of dynamical properties can be rectified on using hybrid atomic orbitals; the standard approach to their use is to take linear combinations of the atomic orbitals. The method is justified *a posteriori* according to a qualitative agreement between, for instance, the hybrid directions and molecular geometry. The main weakness of this approach is that hybridization is imposed on an isolated atom in an arbitrary way – the linear transformations used are not seen to emerge in a natural way from the physics of an atom in a molecular environment [9].

In the present communication we show that two one-dimensional ordinary-differential equations obtained after separation of variables in the Schrödinger equation applied to the hydrogen atom in prolate spheroidal coordinates are related to Heun's confluent equation. The quasi-radial and quasi-angular functions can hence be represented in terms of confluent Heun functions. Our purpose is first to discover a direct method of solution of the Schrödinger equation and to obtain the complete set of CSF in a closed algebraic form, and second to demonstrate that CSF are hybrid orbitals that reproduce the dynamical properties of atomic orbitals, and therefore these functions are the most appropriate basic functions for diatomic molecular calculations. We concentrate on the separation and solution of the partial-differential equations, making no use of other and sophisticated methods such as using a purported *hidden symmetry* of the hydrogen atom, or a group-theoretical approach. The developed method of solution, with the wave functions of the hydrogen atom written in spheroidal coordinates, can be included in textbooks of quantum mechanics and quantum chemistry as an example of *naturally* obtained hybrid functions that reflect the dynamical properties of atomic orbitals. The graphs of CSF for varied R make visible these dynamical properties.

The article is organized as follows. After stating the purpose, we present briefly the basic equations in section 2. Section 3 reveals the relation of CSF to confluent Heun functions and presents explicit expressions for the introduced functions. Section 4 presents illustrations of spheroidal

functions and reveals their properties, before a conclusion in section 5. Atomic units in which $e = m = \hbar = 1$, are used throughout this article.

2. Basic equations

We consider a general one-electron atom with nuclear charge Z . Because the energy spectrum is independent of the system of coordinates in which the electron motion is quantized, the problem becomes reduced to the derivation of the amplitude functions. The amplitude function in prolate spheroidal coordinates $\xi = (r_a + r_b) / R$, $\eta = (r_a - r_b) / R$, $\varphi = \arctan(y / x)$ is represented as this product of three functions

$$\psi(\xi, \eta, \varphi) = X(\xi)Y(\eta)e^{\pm im\varphi}, \tag{1}$$

in which the quasi-radial $X(\xi)$ and quasi-angular $Y(\eta)$ functions depend upon distance R between the foci of spheroidal coordinates; one centre, at left, has charge Z , and another, a dummy centre at right, has $Z = 0$. In the definition of the spheroidal variables, r_a and r_b denote the distances of an electron from those left and right foci of spheroidal coordinates, respectively. A surface of constant ξ is an ellipsoid; a surface of constant η is a hyperboloid. These variables ξ and η are thus defined in distinct domains $1 \leq \xi < \infty$ and $-1 \leq \eta \leq 1$, with $0 \leq \varphi \leq 2\pi$.

Substituting (1) into the Schrödinger equation for one-electron atom, one obtains that $X(\xi)$ and $Y(\eta)$ satisfy these equations

$$\frac{d}{d\xi}(\xi^2 - 1)\frac{dX}{d\xi} + \left[\lambda + \frac{ER^2}{2}(\xi^2 - 1) + ZR\xi - \frac{m^2}{\xi^2 - 1} \right] X = 0, \tag{2a}$$

$$\frac{d}{d\eta}(1 - \eta^2)\frac{dY}{d\eta} + \left[-\lambda + \frac{ER^2}{2}(1 - \eta^2) - ZR\eta - \frac{m^2}{1 - \eta^2} \right] Y = 0, \tag{2b}$$

in which appear separation parameter λ ; $E = -Z^2 / 2n^2$ is the electron energy in which n denotes the principal quantum number.

Equations (2) imply that functions $X(\xi) \equiv W(t)$ and $Y(\eta) \equiv W(t)$ satisfy the same equation with distinct domains for the variables

$$\frac{d}{dt}(1 - t^2)\frac{dW}{dt} - \left[\lambda - \frac{Z^2R^2}{4n^2}(1 - t^2) + ZRt + \frac{m^2}{1 - t^2} \right] W = 0. \tag{3}$$

Representing $W(t)$ as

$$W(t) = e^{-\frac{ZR(t-1)}{2n}} (t^2 - 1)^{\frac{m}{2}} \Phi(t), \quad (t = \xi) \tag{4a}$$

$$W(t) = e^{-\frac{ZR(1+t)}{2n}} (1 - t^2)^{\frac{m}{2}} \Phi(t), \quad (t = \eta) \tag{4b}$$

and substituting (4a) and (4b) into (3), we obtain an equation for unknown function $\Phi(t)$

$$\begin{aligned} (1 - t^2)\frac{d^2\Phi}{dt^2} - \left[2(m+1)t + \frac{ZR}{n}(1 - t^2) \right] \frac{d\Phi}{dt} \\ - \left[\lambda + m^2 + m + \frac{ZR}{n}(n - m - 1)t \right] \Phi = 0. \end{aligned} \tag{5}$$

The resolution of the problem becomes reduced to the solution of one-dimensional Eq. (5).

In CSF (1) occur spheroidal quantum numbers (n_ξ, n_η, m) , of which n_ξ denotes the number of nodes of quasi-radial function $X_{n_\xi m}(\xi)$ in domain $[1, \infty)$; n_η denotes the number of nodes of quasi-angular function $Y_{n_\eta m}(\eta)$ in domain $[-1, 1]$.

3. Relation to confluent Heun equation

In its standard canonical normal form, Heun’s differential equation is expressed as [13-15]

$$\left\{ x(x-1)(x-\mu) \frac{d^2}{dx^2} + [c(x-1)(x-\mu) + dx(x-\mu) + (a+b+1-c-d)x(x-1)] \frac{d}{dx} + (abx - \alpha) \right\} \chi(x) = 0. \tag{6}$$

This equation has three regular singularities $x=0$, $x=1$, $x=\mu$ and one irregular singularity $x=\infty$; a , b , c , d are local parameters; μ is a scaling parameter that determines the location of one singular point; α is an accessory parameter that typically plays a role of spectral parameter.

Heun’s singly confluent equation is obtained from general Heun Eq. (6) through confluence – a coalescence of two singularities, implemented on redefining parameters and taking limits. Coalescing singular points $x=0$ and $x=\infty$, with $\mu=1/\varepsilon$, $b=p/\varepsilon$, $\alpha=\beta/\varepsilon$, $\varepsilon \rightarrow 0$, $p=\mu$, $\beta=a$, we obtain [14,15]

$$\left\{ x(x-1) \frac{d^2}{dx^2} + [c(x-1) + dx - \mu x(x-1)] \frac{d}{dx} - (a\mu x - \alpha) \right\} \chi(x) = 0. \tag{7}$$

Performing Möbius transformation $x \rightarrow t$ with $t=2x-1$, Heun’s confluent Eq. (7) becomes expressed as [15]

$$\left\{ (1-t^2) \frac{d^2}{dt^2} - \left[(c+d)t - c + d + \frac{\mu}{2}(1-t^2) \right] \frac{d}{dt} - \left[\alpha - \frac{\mu a}{2}(1+t) \right] \right\} \chi(t) = 0. \tag{8}$$

Assuming that

$$\begin{aligned} a &= -n + m + 1, \\ c &= d = m + 1, \\ \mu &= 2ZR / n, \\ \alpha &= \lambda + m^2 + m - ZR(n - m - 1) / n, \end{aligned} \tag{9}$$

Eq. (8) converts into Eq. (5). The solutions of confluent Heun Eq. (8) with parameters defined in Eq. (9) should hence coincide with the solutions of Eq. (5), $\Phi(t) = \chi(x)$ in which $x = (t+1)/2$.

For any singular points $x=0$, $x=1$ and $x=\infty$, two solutions of Eq. (7) exist and are characterized by the particular behaviour at these singular points [15]. As shown in [1], the solution of Eq. (5) is expected to be polynomial; we hence seek the solution of Heun’s confluent Eq. (7) in a polynomial form. Near singular point $x=0$, the regular solution is represented as an expansion in a power series,

$$\chi(x) = \sum_{i=0}^s g_i x^i, \quad g_0 = 1, \quad x = (t+1)/2. \tag{10}$$

Here s defines the degree of the polynomial and g_i are polynomial coefficients that depend on R . For the non-polynomial solutions of Eq. (7), the algorithm of the calculation is discussed elsewhere [14,15].

For polynomial (10) to be a solution of Eq. (7), the coefficients in (10) must satisfy a three-term recurrence relation [15]

$$(i+1)(i+c)g_{i+1} - [i(i+c+d+\mu-1)+\alpha]g_i + \mu(i+a-1)g_{i-1} = 0. \tag{11}$$

When parameters a, c, d, μ and accessory parameter α are defined with Eq. (9), Eq. (11) transforms into this three-term recurrence relation

$$(i+1)(i+m+1)g_{i+1} + \left[\frac{ZR}{n}(n-m-1) + s(2m+s+1) - h \right. \\ \left. - i \left(i + 2m + 1 + \frac{2ZR}{n} \right) \right] g_i - \frac{2ZR}{n}(n-m-i)g_{i-1} = 0, \tag{12}$$

in which the relation of h to λ is $h = \lambda + (m+s)(m+s+1)$. Recurrence relation (12) determines the polynomial coefficients in (10) and yields an equation for new separation parameter h . When $R \rightarrow 0$, (12) transforms into a two-term recurrence relation that leads to the well-known solutions [1] of the radial and angular equations.

When $s = 0$, (10) is a polynomial of degree zero; recurrence relation (12) converts into the equation $(ZR/n)(n-m-1) - h = 0$. To satisfy this equation for arbitrary R , conditions $n = m + 1$ and $h = 0$ must be fulfilled; we accordingly obtain one spheroidal function $\psi_{n_\xi n_\eta m}$ with quantum numbers $n_\xi = n_\eta = 0$. When $s = 1$, (10) converts into a polynomial of first degree; recurrence relation (12) yields a quadratic equation for h , which has two real and distinct roots, $h_1 < h_2$. As a result, we derive two spheroidal functions ψ_{01m} ($h = h_1$) and ψ_{10m} ($h = h_2$) with $n = m + 2$. When $s = 2$, (10) converts into a polynomial of second degree; recurrence relation (12) yields a cubic equation for h , which has three real and distinct roots, $h_1 < h_2 < h_3$. We obtain three spheroidal functions ψ_{02m} ($h = h_1$), ψ_{11m} ($h = h_2$) and ψ_{20m} ($h = h_3$) with $n = m + 3$. When $s = 3$, (10) converts into a polynomial of third degree and (12) yields an equation of fourth degree for h , which has four real and distinct roots, $h_1 < h_2 < h_3 < h_4$. The corresponding spheroidal functions are: ψ_{03m} ($h = h_1$), ψ_{12m} ($h = h_2$), ψ_{21m} ($h = h_3$) and ψ_{30m} ($h = h_4$) with $n = m + 4$. Polynomials of fourth, fifth... degrees and the equations for appropriate separation parameters are readily evaluated. For given n and m , h is thus a solution of an equation of order $(n - m)$ that has $(n - m)$ real and distinct roots.

To summarize the above results, we state that, for given m and s ($s \equiv n - m - 1 = 0, 1, 2, \dots$) the CSF are expressible as

$$\psi_{n_\xi n_\eta m} = C_{n_\xi n_\eta m} e^{\frac{ZR(\xi+\eta)}{2n}} \left[(\xi^2 - 1)(1 - \eta^2) \right]^{\frac{m}{2}} \sum_{i=0}^m g_i \left(\frac{\xi+1}{2} \right)^i \sum_{j=0}^s g_j \left(\frac{\eta+1}{2} \right)^j e^{\pm im\varphi}, \tag{13}$$

in which

$$g_0 = 1, \\ g_i = \frac{1}{i(m+1)} \left\{ \left[h - (s+1-i)(2m+s+i) - (s+2-2i)\frac{ZR}{n} \right] g_{i-1} \right. \\ \left. + \left[2(s+2-i)\frac{ZR}{n} \right] g_{i-2} \right. \quad (i = 1, 2, \dots, s) \tag{14}$$

Here h is solution of the algebraic equation of order $(n - m)$

$$\left(h + s \frac{ZR}{n} \right) g_s + \frac{2ZR}{n} g_{s-1} = 0, \quad (s = 0, 1, \dots) \tag{15}$$

and $C_{n_\xi n_\eta m}$ is a normalizing factor.

We proceed to establish the relations between quantum numbers n_ξ, n_η, m used to specify the electronic states in the general case (with R finite and nonzero) and spherical quantum numbers

n, l, m and paraboloidal quantum numbers n_1, n_2, m describing the hydrogenic states at $R = 0$ and $R \rightarrow \infty$, respectively. Employing that the number of nodal surfaces of $X_{n_\xi m}(\xi)$ and $Y_{n_\eta m}(\eta)$ functions is conserved as R varies [16], we obtain that $n - l - 1 = n_\xi = n_1$ and $l - m = n_\eta = n_2$. The spheroidal quantum numbers corresponding to degenerate states with given n and m are hence related according to a condition that $n = n_\xi + n_\eta + m + 1$.

Spheroidal functions (13) correspond to a location of a nucleus at the left centre of spheroidal coordinates ($\xi = 1, \eta = -1$). For a nucleus located at the right centre ($\xi = 1, \eta = 1$), the quasi-radial function $X_{n_\xi m}(\xi)$ remains unchanged, whereas $\eta \rightarrow -\eta$ (or equivalently $\vec{r}_a \square \vec{r}_b$) in the quasi-angular function $Y_{n_\eta m}(\eta)$. We thus obtain that Eqs. (13) - (15) define a set of CSF on each centre of spheroidal coordinates for the description of localized bonds.

4. Properties of Coulomb spheroidal functions

CSF (13) with varied m are orthogonal because of factor $\exp(\pm im\varphi)$. Functions $X_{n_\xi m}(\xi)$ and $Y_{n_\eta m}(\eta)$ are defined with Eq. (5), in which separation parameter λ plays the role of an eigenvalue. The solutions of this equation corresponding to a degenerate level with given n and m are hence mutually orthogonal, provided only that λ are distinct. We recall from section 3 that h , and accordingly λ , are all real and distinct. Hence $\langle X_{n_\xi m} | X_{n_\xi m} \rangle = 0$ and $\langle Y_{n_\eta m} | Y_{n_\eta m} \rangle = 0$ if $n_\xi + n_\eta = n'_\xi + n'_\eta$ and $n'_\xi \neq n_\xi$, $n'_\eta \neq n_\eta$.

Spheroidal functions $\psi_{n_\xi n_\eta m}(\xi, \eta, \varphi)$ are representable as linear combinations of Coulomb spherical functions $\Psi_{nlm}(r_a, \vartheta_a, \varphi)$. This result is achievable on representing r_b as $r_b = (r_a^2 - 2r_a R \cos \vartheta_a + R^2)^{1/2}$, in which ϑ_a denotes the angle between radius vector \vec{r}_a and polar axis z , and on representing spheroidal coordinates $\xi = (r_a + r_b) / R$ and $\eta = (r_a - r_b) / R$ through spherical ones $(r_a, \vartheta_a, \varphi)$ in $\psi_{n_\xi n_\eta m}(\xi, \eta, \varphi)$. Performing the appropriate calculation, we obtain that, at all separations, $\psi_{n_\xi n_\eta m}(\xi, \eta, \varphi)$ is a linear combination of spherical functions $\Psi_{nlm}(r_a, \vartheta_a, \varphi)$ with principal quantum number $n = n_\xi + n_\eta + m + 1$ and orbital quantum number $l = m, m + 1, \dots, n - 1$. The normalized spheroidal functions are thus expressible as

$$\psi_{n_\xi n_\eta m} = \sum_{l=m}^{n-1} A_{nlm}(R) \Psi_{nlm}(r_a, \vartheta_a, \varphi), \tag{16}$$

in which expansion coefficients A_{nlm} are related with a condition $\sum_{l=m} A_{nlm}^2 = 1$. When $R \rightarrow 0$, one expansion coefficient is equal to unity in (16) whereas the others tend to zero. When $R \rightarrow \infty$, spheroidal function $\psi_{n_\xi n_\eta m}$ converts into paraboloidal function $\psi_{n_1 n_2 m}$ with $n_1 = n_\xi$ and $n_2 = n_\eta$. Equation (16) accordingly transforms into the relation between Coulomb paraboloidal and Coulomb spherical functions [1]. In this limit, we hence write that $A_{nlm}(\infty) = \langle j_1 j_2 \mu_1 \mu_2 | lm \rangle$ in which $j_1 = j_2 = (n - 1) / 2$, $\mu_1 = (m + n_\xi - n_\eta) / 2$, $\mu_2 = (m - n_\xi + n_\eta) / 2$; $\langle j_1 j_2 \mu_1 \mu_2 | lm \rangle$ is a Clebsch-Gordan coefficient. At arbitrary separation R and with $n - m \leq 3$, explicit expressions for $\psi_{n_\xi n_\eta m}$ are presented in the appendix. We thus obtain that, with the exception of ψ_{00m} , the introduced CSF are hybrid functions composed of Coulomb spherical functions Ψ_{nlm} corresponding to the degenerate level

with $E_n = -Z^2 / 2n^2$ and $n = n_\xi + n_\eta + m + 1$. In (16), the hybridization coefficients are determined uniquely by distance R from a nucleus to a dummy centre.

The expression for the probability density is obtained from Eq. (16). Taking into account that spherical function Ψ_{nlm} is a product of radial function $R_{nl}(r_a)$ and spherical harmonic $Y_{lm}(\mathcal{G}_a, \varphi)$, we derive

$$\rho_{n_\xi n_\eta m}(r_a, \mathcal{G}_a) = \sum_{l, l'=m}^{n-1} A_{nlm} A_{n'l'm} R_{nl}(r_a) R_{n'l'}(r_a) Y_{lm}^*(\mathcal{G}_a, \varphi) Y_{l'm}(\mathcal{G}_a, \varphi). \quad (17)$$

The radial and angular probability densities are derived on integrating (17) over either spherical angles \mathcal{G}_a and φ or radius r_a , which gives

$$\rho_{n_\xi n_\eta m}(r_a) = \sum_{l=m}^{n-1} A_{nlm}^2 R_{nl}^2(r_a), \quad (18)$$

for radial density and

$$\rho_{n_\xi n_\eta m}(\mathcal{G}_a) = \sum_{l=m}^{n-1} A_{nlm}^2 |Y_{lm}(\mathcal{G}_a, \varphi)|^2, \quad (19)$$

for angular density, respectively.

An important property that follows from Eq. (17) is that the contribution of each spherical orbital to a spheroidal one depends on distance R from the nucleus to the dummy centre, and varies appreciably with R . The shape of hybrid orbital $\psi_{n_\xi n_\eta m}$ with $n_\xi + n_\eta > 0$ depends in turn on the location of the dummy centre. As a graphic illustration of this dependence, we display the probability density $\rho_{n_\xi n_\eta m}(r_a, \mathcal{G}_a)$ with r_a fixed and distance R increasing along axis z from the spherical polar limit at $R = 0$ to the paraboloidal limit as $R \rightarrow \infty$. To reveal the stretching effect, we take r_a to be equal to the size of shell r_n of the hydrogenic state under consideration, i.e. $r_a = r_n \square n^2 / Z$ in $\rho_{n_\xi n_\eta m}(r_a, \mathcal{G}_a)$. Figures 1-5 are polar plots of angular probability density for spheroidal hybrid orbitals with $m = 0$, $n_\xi + n_\eta \leq 3$ and $Z = 1$.

Figure 1 shows that, at $R = 0$, the shape of spheroidal orbital ψ_{010} coincides with the shape of spherical polar orbital Ψ_{2p0} . When R increases, this shape alters such that the negative lobe contracts monotonically along axis z , whereas the positive lobe expands along axis z ; when R exceeds $r_a = n^2 / Z = 4$, the positive lobe contracts slightly. When $R \square 1$, the negative lobe is much smaller than the positive lobe. When $R \rightarrow \infty$, the shape of spheroidal orbital ψ_{010} resembles strongly the shape of paraboloidal orbital with quantum numbers $n_1 = 0$ and $n_2 = 1$.

At $R = 0$, the shape of spheroidal orbital ψ_{100} has central symmetry as shown in Fig. 2, and coincides with the shape of spherical polar orbital Ψ_{2s} . When R increases, the spheroidal orbital ψ_{100} has its centre clearly displaced along negative axis z . When $R \square 1$, the shape of spheroidal orbital ψ_{100} resembles strongly the shape of paraboloidal orbital with quantum numbers $n_1 = 1$ and $n_2 = 0$. According to Figs. 1 and 2, at $R \square 1$ the shapes of spheroidal orbitals ψ_{010} and ψ_{100} are practically identical, but oriented oppositely along axis z .

Figures 3, 4 and 5 show the angular probability density for spheroidal hybrid orbitals ψ_{020} , ψ_{200} and ψ_{030} as distance R increases from $R = 0$ to $R \square 1$. At $R = 0$, the shapes of these spheroidal orbitals coincide with the shape of spherical orbitals Ψ_{3d0} , Ψ_{3s} and Ψ_{4f0} . When $R \square 1$, the shapes of spheroidal orbitals ψ_{020} , ψ_{200} and ψ_{030} resemble strongly the shapes of paraboloidal orbitals with quantum numbers $(n_1 = 0, n_2 = 2)$, $(n_1 = 2, n_2 = 0)$ and $(n_1 = 0, n_2 = 3)$, respectively. Other tendencies analogous to those shown in Figs. 1 and 2 are also observable in Figs. 3-5.

For the angular probability density when r_a is much less than the size of the shell, i.e. when $r_a \ll n^2 / Z$ in $\rho_{n_\xi n_\eta m}(r_a, \mathcal{G}_a)$, we refrain from presenting the appropriate angular probability density because the transformation of shapes is simply opposite to that when $r_a = n^2 / Z$. Explicitly, when R increases from $R=0$ to $R \ll 1$, the positive lobes contract as the negative lobes expand. As follows from Figs. 6 and 7, angular probability density $\rho_{n_\xi n_\eta m}(r_a, \mathcal{G}_a)$ that is integrated over radius r_a is equally squeezed or stretched along positive and negative axis z . According to Fig. 6 presented in [10], because angular probability distributions are equalized at $\mathcal{G}_a = 0$, the stretching or squeezing effects are unobservable.

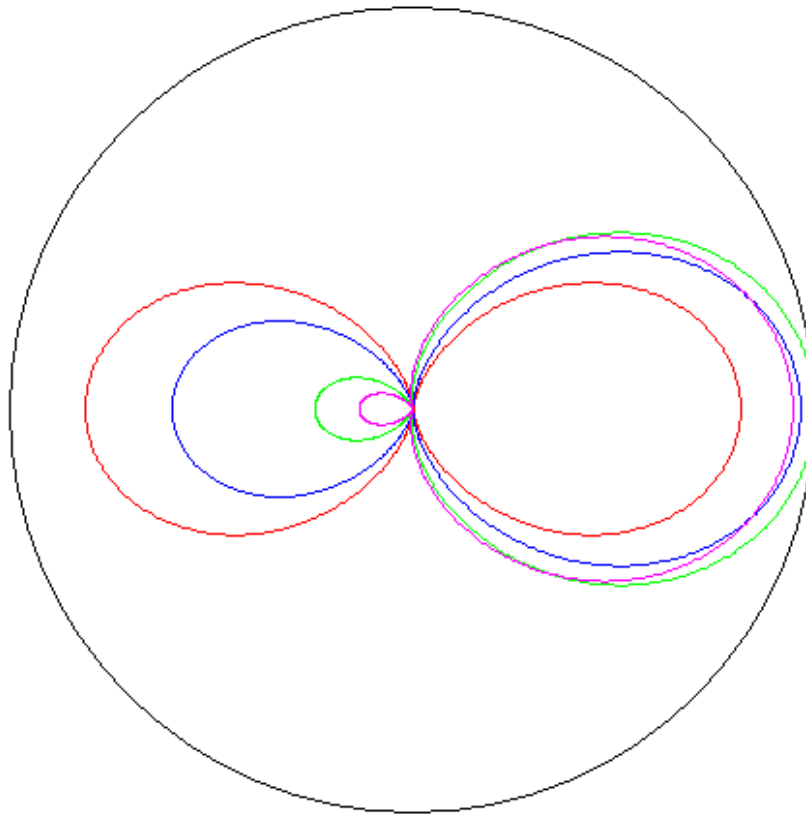


Fig. 1 Polar plots of angular probability density $\rho_{010}(r_a, \mathcal{G}_a)$ at $Z=1$ and $r_a = 4$. Distance R from a nucleus to the dummy centre is $R=0$ (red curve), $R=1$ (blue curve), $R=5$ (green curve) and $R=20$ (magenta curve). Axis z is horizontal.

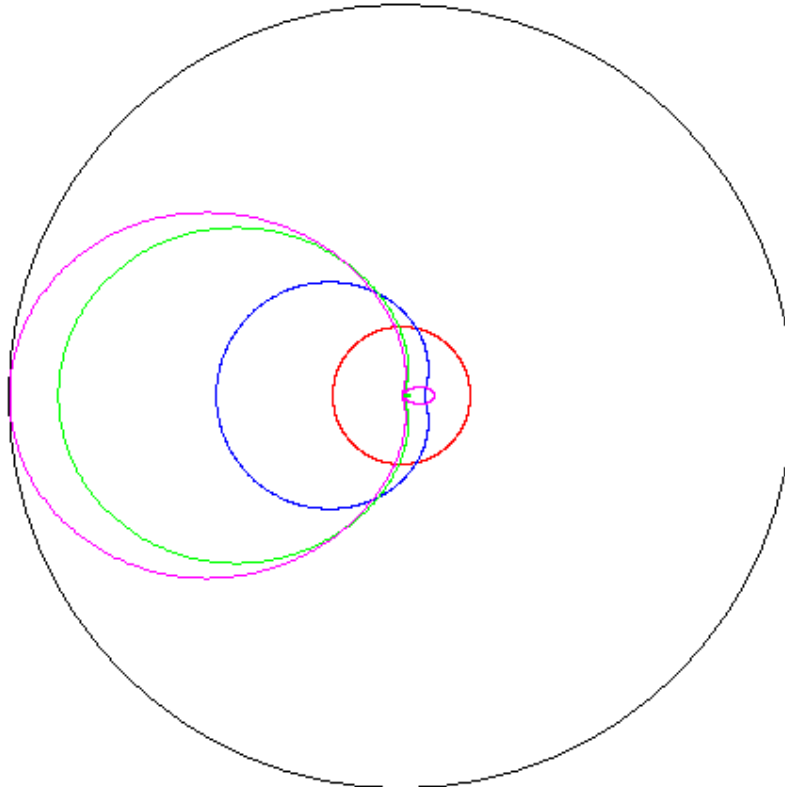


Fig. 2 As in Fig. 1 but for $\rho_{100}(r_a, \mathcal{G}_a)$ at $r_a = 4$.

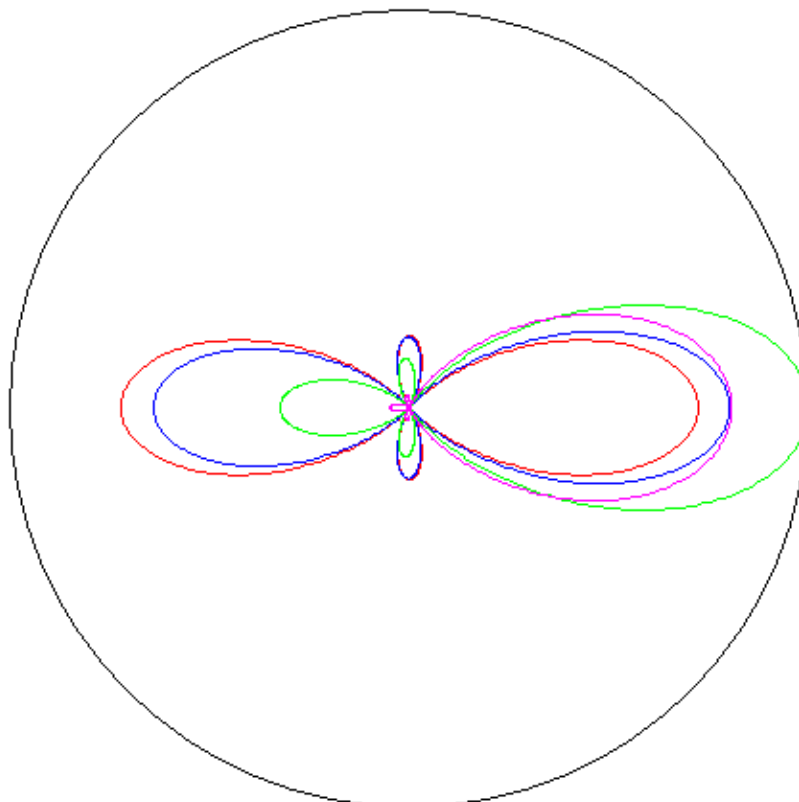


Fig. 3 As in Fig. 1 but for $\rho_{020}(r_a, \mathcal{G}_a)$ at $r_a = 9$.

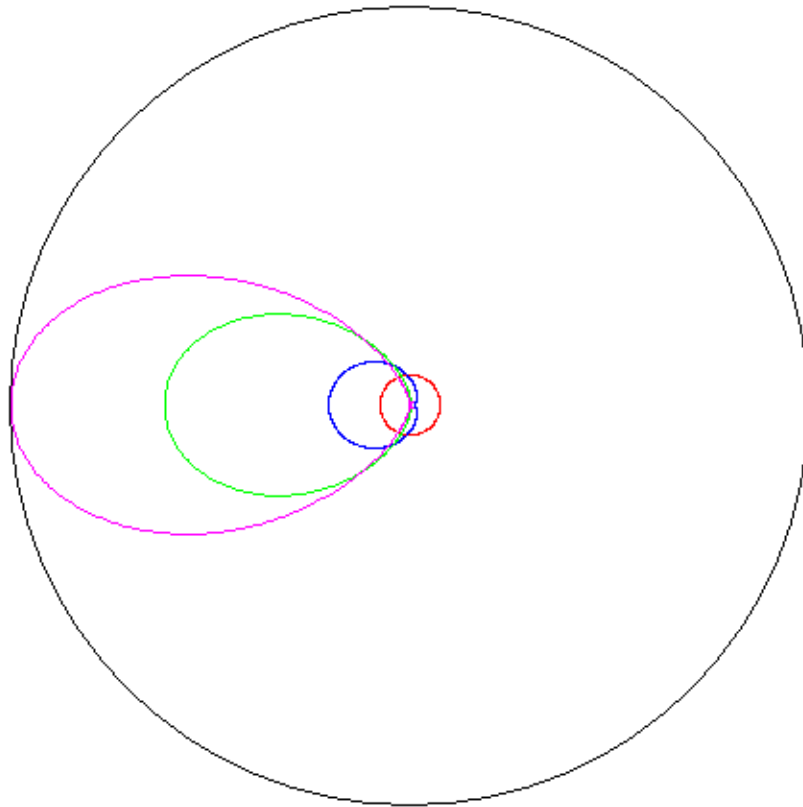


Fig. 4 As in Fig. 1 but for $\rho_{200}(r_a, \mathcal{G}_a)$ at $r_a = 9$.

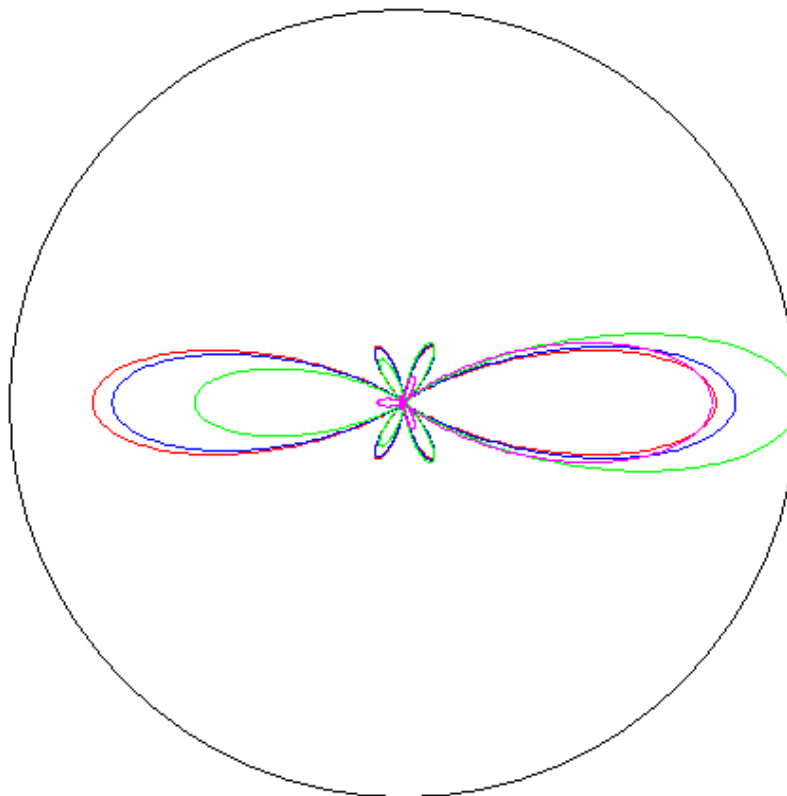


Fig. 5 As in Fig. 1 but for $\rho_{030}(r_a, \mathcal{G}_a)$ at $r_a = 16$.

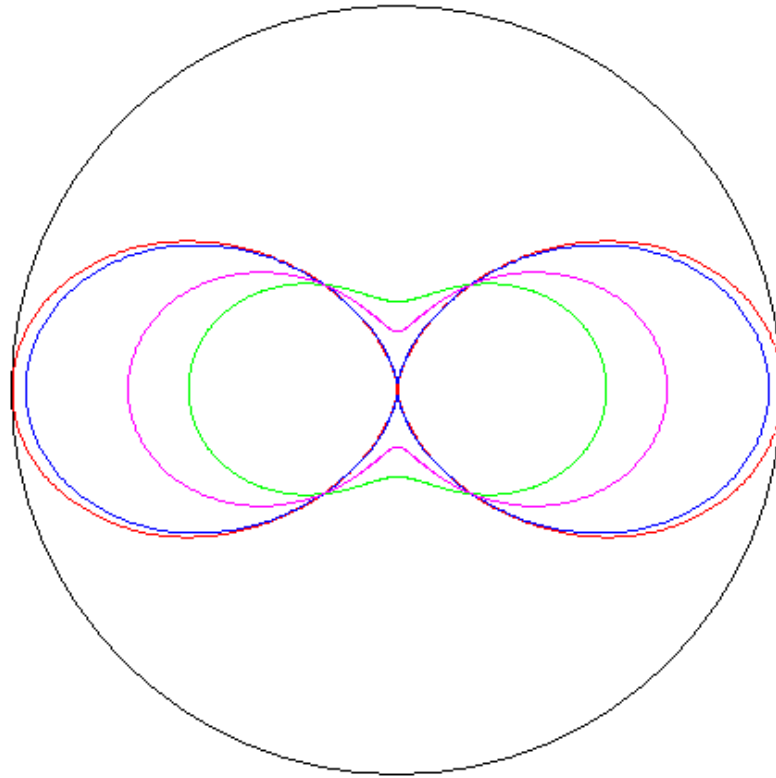


Fig. 6 Polar plots of angular probability density $\rho_{010}(\mathcal{G}_a)$ at $Z=1$. The distance R from a nucleus to the dummy centre is: $R=0$ (red curve), $R=1$ (blue curve), $R=5$ (green curve) and $R=20$ (magenta curve). The axis z is horizontal.

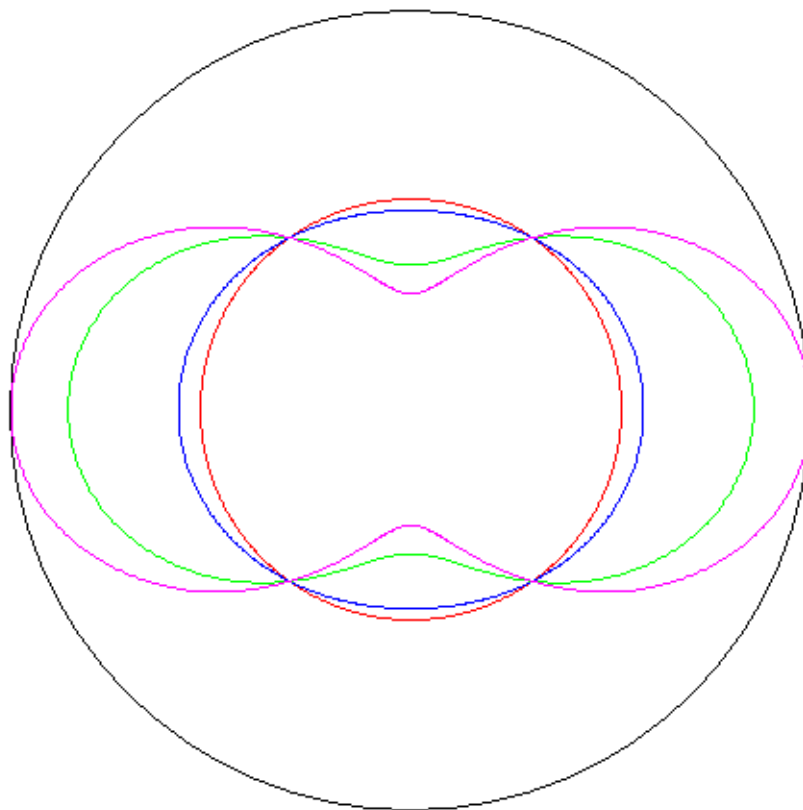


Fig. 7 As in Fig. 6 but for $\rho_{100}(\mathcal{G}_a)$.

5. Conclusion

Our treatment of the hydrogen atom in prolate spheroidal coordinates demonstrates that the Coulomb spheroidal functions are related to the solutions of Heun's confluent equation, which enables us to present CSF in a closed algebraic form. Unlike hydrogen molecular ion H_2^+ , for which the wave functions are not expressible in a polynomial form, the wave functions for the hydrogen atom in spheroidal coordinates are expressible as the polynomial solutions of Heun's confluent equation. For given principal quantum number n and magnetic quantum number m the quasi-radial $X_{n_\xi m}(\xi)$ and quasi-angular $Y_{n_\eta m}(\eta)$ wave functions are polynomials of order $n-m-1$. CSF with different n and m but the same $n-m$ or $n_\xi + n_\eta$ are thus products of two similar polynomials defined in distinct regions of variables ξ and η , as follows from Eq. (13).

We explore the properties of spheroidal orbitals; for $R > 0$ they are hybrid orbitals composed of spherical wave functions. An important result is that the angular probability density depends on the distance from a nucleus to the dummy centre, and varies substantially with R . For given n and m , the orbital most stretched toward the dummy centre is an orbital with quasi-angular nodes of maximum number, whereas the orbital most stretched in the opposite direction is an orbital with quasi-radial nodes of maximum number. An orbital with $n_\eta = n-m-1$ is hence a bonding orbital, whereas an orbital with $n_\xi = n-m-1$ is an antibonding orbital. The characteristic feature of CSF is thus the development of preferred directions around an atom, i.e. the bond directions. These features reveal the great advantage of a Coulomb spheroidal basis over a Coulomb spherical basis in calculations on diatomic molecules. Our calculations [17,18] undertaken for H_2^+ show that the similarity of the one- and two-Coulomb-centre wave functions in spheroidal coordinates, combined with effective convergence properties of CSF, makes the calculated results substantially nearer the exact ones.

The most striking feature of Rydberg states of long-range diatomic molecules predicted in [19] is that some molecular Rydberg states possess large electric-dipolar moments, which, in any long-lived molecular state, presents a promising opportunity for manipulation and control through the application of an electric field. A simple model of these molecules has been elaborated: Rydberg states are described with a sum of degenerate Coulomb elliptic wave functions; the attraction between a weakly bound electron and a ground-state atom is described with a short-range potential [11]. In this way, many qualitative features have been understood. CSF are ideal zero-order functions for the investigation of Rydberg states of diatomic molecules and molecular ions. To obtain more precise, quantitative results, Rydberg states must be described with CSF; the attraction between a weakly bound electron and two atomic cores should be treated using a realistic potential. Other applications of CSF are discussed elsewhere [10].

Appendix

Here we represent some spheroidal functions $\psi_{n_\xi n_\eta m}$ in terms of spherical functions Ψ_{nlm} :

$$\psi_{00m} = \Psi_{m+1mm}, \tag{A.1}$$

$$\psi_{01m} = \left(1 + (nh_1 / ZR)^2\right)^{-1/2} \left[\frac{nh_1}{ZR} \Psi_{m+2mm} + \Psi_{m+2m+1m} \right], \tag{A.2}$$

$$\psi_{10m} = \left(1 + (nh_2 / ZR)^2\right)^{-1/2} \left[\frac{nh_2}{ZR} \Psi_{m+2mm} + \Psi_{m+2m+1m} \right],$$

$$\begin{aligned}
\psi_{02m} &= C_{02m} \left[\sqrt{\frac{m+2}{m+1}} \frac{h_1}{(h_1 - 4m - 6)} \Psi_{m+3mm} + \sqrt{\frac{2m+3}{m+1}} \frac{nh_1}{2ZR} \Psi_{m+3m+1m} \right. \\
&\quad \left. + \Psi_{m+3m+2m} \right], \\
\psi_{11m} &= C_{11m} \left[\sqrt{\frac{m+2}{m+1}} \frac{h_2}{(h_2 - 4m - 6)} \Psi_{m+3mm} + \sqrt{\frac{2m+3}{m+1}} \frac{nh_2}{2ZR} \Psi_{m+3m+1m} \right. \\
&\quad \left. + \Psi_{m+3m+2m} \right], \\
\psi_{20m} &= C_{20m} \left[\sqrt{\frac{m+2}{m+1}} \frac{h_3}{(h_3 - 4m - 6)} \Psi_{m+3mm} + \sqrt{\frac{2m+3}{m+1}} \frac{nh_3}{2ZR} \Psi_{m+3m+1m} \right. \\
&\quad \left. + \Psi_{m+3m+2m} \right].
\end{aligned} \tag{A.3}$$

In (A.2), h_1, h_2 are the solutions of a quadratic equation; in (A.3) h_1, h_2, h_3 are the solutions of a cubic equation defined in (15).

References

1. L. D. Landau and E. M. Lifshitz, Quantum mechanics: Non-Relativistic Theory (Oxford UK, Pergamon, 1977)
2. W. Pauli, Ann. Phys. (1922) **68**, 177-240
3. A. H. Wilson, Proc. Roy. Soc. London (1928) **A118**, 617-635
4. A. H. Wilson, Proc. Roy. Soc. London (1928) **A118**, 635-647
5. E. Teller, Z. Physik (1930) **61**, 458-480
6. D. R. Bates and R. H. G. Reid, in "Advances in Atomic and Molecular Physics", v. IV, (Ed. D. R. Bates and I. Esterman, New York USA, Academic Press, 1968)
7. J. D. Power, Phil. Trans. Roy. Soc. London (1973) **A274**, 663-702
8. C. A. Coulson and P. D. Robinson, Proc. Phys. Soc. (1958) **71**, 815-827
9. D. B. Cook and P. W. Fowler, Am. J. Phys. (1981) **49**, 857-867
10. S. M. Sung and D. R. Herschbach, J. Chem. Phys. (1991) **95**, 7437-7448
11. B. E. Granger, E. L. Hamilton, C. H. Greene, Phys. Rev. (2001) **A 64**, 042508
12. T. Kereselidze, Z. S. Machavariani and G. Chkadua, Eur. Phys. J. D. (2011) **63**, 81-87
13. K. Heun, Math. Ann. (1889) **33**, S. 161-179
14. S. Yu. Slavyanov, W. Lay and A. Seeger, Classification // Heun's Differential Equations (Ed: A. Ronveaux, Oxford UK, Oxford University Press, 1995)
15. S. Yu. Slavyanov and W. Lay, Special Functions // A United Theory Based on Singularities (Oxford UK, Oxford University Press, 2000)
16. P. M. Morse and E. C. G. Stueckelberg, Phys. Rev. (1929) **33**, 932-947
17. T. Kereselidze, G. Chkadua and P. Defrance, Mol. Phys. (2015) **113**, 3471-3479
18. T. Kereselidze, G. Chkadua and J. F. Ogilvie, Mol. Phys. (2016) **114**, 148-161
19. C. H. Greene, A. S. Dickinson and H. R. Sadeghpour, Phys. Rev. Lett. (2000) **85**, 2458

Article received: 2016-11-17